

Non-Gaussian statistics of wind pressure processes on a double-layer reticulated shell

*M.F. Huang¹⁾, Teng Li²⁾, He Feng²⁾ and Wenjuan Lou³⁾

^{1), 2), 3)} Institute of Structure Engineering, Zhejiang University, Hangzhou 310058, China
¹⁾ mfhuang@zju.edu.cn

ABSTRACT

Based on the wind tunnel test of rigid model of a double-layer reticulated shell structure, high-order statistics of pressure processes in long time duration were quantified in terms of skewness and kurtosis. It was found that the estimation of kurtosis is sensitive to the duration of wind pressure time-history data. Depending on whether the kurtosis is larger or smaller than three, non-Gaussian random processes can be classified as softening or hardening processes. Hardening load processes with kurtosis values smaller than three were observed in samples of wind pressure acting on the flow reattachment zones. Non-Gaussian peak factors of wind pressure, particularly for those observed hardening pressure process, were calculated by employing various state-of-the-art methods and compared to the direct statistical analysis of the measured long-duration wind pressure data. Furthermore, a mixture distribution model is introduced into the existing translated-peak-process (TPP) method for better modeling the tail and bulk probability regions of a parent distribution.

1. INTRODUCTION

Many researchers have carried out investigations for the non-Gaussian statistics of wind pressure processes based on the translation process theory (Sadek and Simiu, 2002; Tieleman et al., 2006; Kwon and Kareem, 2011; Huang et al., 2013; Yang et al., 2013; Peng et al., 2014). Two common approaches of translation methods are found in literatures. One type is based on the Hermite model and its variant; this type includes Kwon and Kareem's formula (2011), the approximate Hermite model expression proposed in Yang et al. (2013) and Peng et al. (2014). In this type of approach, the non-Gaussian properties of skewness γ_3 and kurtosis γ_4 are used. The second type of approach is based on the point-to-point cumulative distribution function (CDF) mapping procedure from non-Gaussian to Gaussian, with the Sadek-Simiu (SS) procedure (2002) and the recently proposed translated-peak-process (TPP) method (Huang et al., 2013). Whereas the Sadek-Simiu procedure maps extreme values from the Gaussian space to the non-Gaussian space, the TPP method aims to properly model local peak distribution of non-Gaussian processes with the parametric Weibull distribution, from which the peak factor and the fractile level are obtained analytically. The TPP method has the same advantage as the Sadek-Simiu procedure because it

¹⁾ Associate Professor
²⁾ Graduate Student
³⁾ Professor

makes use of all information contained in the time series. Furthermore, the TPP method provides the closed-form solution of peak factors. As long as the Weibull distribution parameters are available, the peak factor and fractile levels of a non-Gaussian process can be analytically evaluated. The possible improvement of the point-to-point mapping approach is the better modeling of parent distribution. Recently, various mixture models have been proposed for the entire distribution function, simultaneously capturing the bulk of the distribution (typically the main mode) with the flexibility of an extreme value model for the upper/lower tails (MacDonald et al. 2011). The mixture models have been used in translation methods to better estimate peak pressure effects (Peng et al. 2014; Ding and Chen 2014). However, the use of a mixture model may not offer a significant improvement over the existing translation methods (Peng et al. 2014). It is necessary to further investigate the effectiveness of the mixture model in the TPP method.

Hermite model-based approaches, including Kwon and Kareem's formula (Kwon and Kareem 2011), the work of Yang et al. (2013) and Peng et al. (2014) have inherent limits due to the use of the Hermite moment model developed by Winterstein (1988). The original Hermite moment model provides a representation of the functional transformation from a Gaussian process to a non-Gaussian softening process defined as the kurtosis γ_4 greater than 3 (Winterstein, 1988). Most of existing Hermite model-based methods or formulas are therefore only applicable to a softening process with a positive excess kurtosis. In the Sadek-Simiu procedure, a gamma distribution was selected to model the parent distribution of a given non-Gaussian process. Because a gamma distribution has a positive excess kurtosis, it cannot be used to describe the parent distribution of a hardening process. To complete the original Hermite moment model for all practical paired values of skewness and kurtosis, several attempts have been made to extend the moment-based Hermite translation model for hardening non-Gaussian processes ($\gamma_4 - 3 < 0$) with empirical formulations for determining the translation model coefficients (Choi and Sweetman 2010; Chen 2014; Ding and Chen 2014). The modeling of translation function for hardening non-Gaussian wind effect processes has not been extensively addressed in literature (Chen 2014; Ding and Chen 2014). Huang et al. 2014 observed hardening wind pressure processes on a long-span roof model tested in the wind tunnel, and proposed an analytical formula for non-Gaussian peak factors of hardening load processes.

Based on the wind tunnel tests, the statistical moments of the wind pressure processes measured on a double-layer reticulated shell roof are evaluated. The sensitivities of high-order statistics to the record duration are studied. A mixture distribution model is introduced that combines an analytical tail distribution with kernel sampling density for the bulk of distribution. With the aid of the mixture model, the Sadek-Simiu procedure and the TPP method are modified in this study. Comparative performance studies have been further carried out to reveal the advantage and disadvantage of various state-of-the-art translation methods, and investigate the effectiveness of mixture model in the Sadek-Simiu procedure and TPP method.

2. WIND TUNNEL EXPERIMENTS

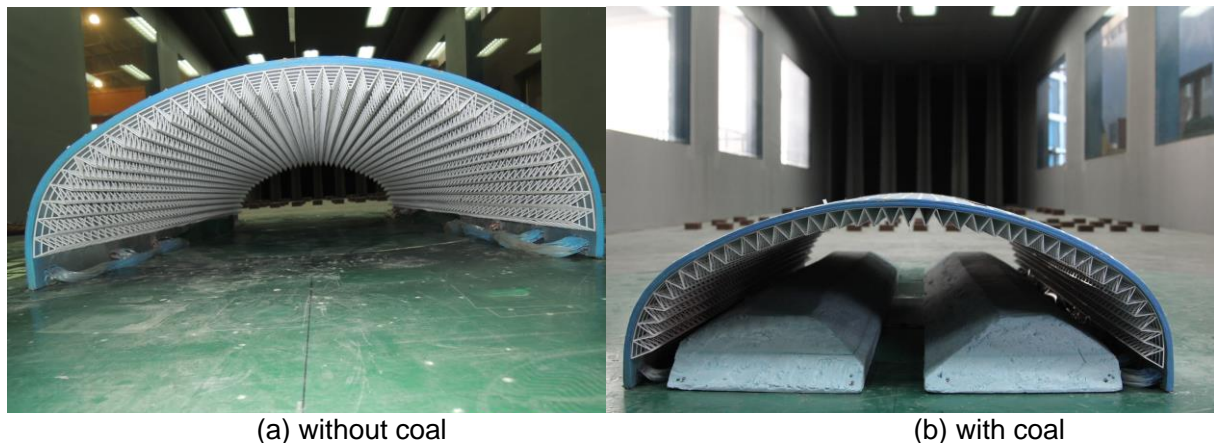
A cylindrical reticulated roof structure with a height of 45 m and a span of 120 m

is planned to construct in a coastal site of China for coal storage. The site is in the A category (open terrain), with a power law exponent of $\alpha = 0.12$ for the mean wind speed profile stipulated in the Chinese Load Code (GB50009-2012). The turbulence intensity profile recommended for the A category is given by the following expression:

$$I_u = I_{10} \left(\frac{Z}{10} \right)^{-\alpha} \quad (1)$$

where Z is the height, $I_{10}=0.12$.

Wind tunnel experiments were carried out in a boundary layer wind tunnel, which has a working cross section 4 m wide \times 3 m high and a length of 18 m. A model of the roof structure was made at a geometric scale of 1:150 with and without coal inside (see Fig. 1). Spires and roughness cube elements were used to simulate the desired boundary layer wind structure following the A category. Wind pressures on the rigid model of the roof shell were measured using a synchronous multi-pressure sensing system (SMPSS). The main roof was covered with densely distributed pressure sensors with a total of 500 pressure taps to quantify the net pressure actions at 250 locations, as shown in Fig.2. At each measuring location, a pair of pressure taps was installed to measure external and internal pressure effects. The wind tunnel test was carried out with a wind speed of 15.4 m/s at the reference height of 1.0 m above the wind tunnel floor. The design wind speed with a return period of 100 years for the construction site is approximately 52.52 m/s at a full-scale height of 150 m. Therefore, the wind speed scale in the wind tunnel experiment was approximately 1/3.4 and the time scale became 1/44. The pressure data were recorded at a sampling frequency of 625 Hz for time duration of 300 s, which is equivalent to 220 minutes in full-scale situations.



(a) without coal (b) with coal
 Fig. 1 Wind tunnel test model of a double-layer reticulated shell

The wind pressure results are presented in terms of the net pressure coefficient, which is defined as follows:

$$C_{pi}(t) = \frac{P_i^{ex}(t) - P_i^{in}(t)}{0.5\rho V_\infty^2} \quad (2)$$

where C_{pi} is the net pressure coefficient for the i th measuring location of the roof; P_i^{ex} and P_i^{in} are the pressure values at the external and internal surfaces of the roof, respectively. The main focus of this study is on the non-Gaussian characteristics and peak factors of the wind effect processes defined in Eq. (2).

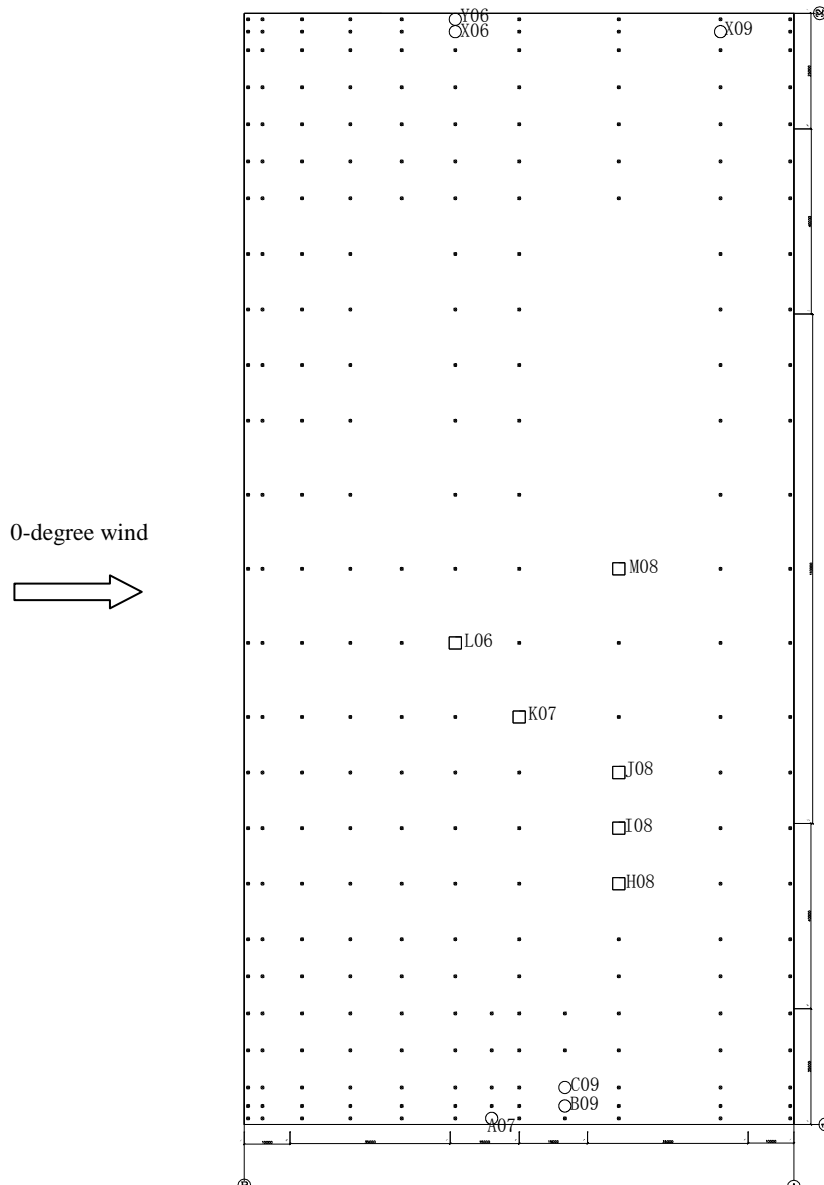


Fig. 2 Arrangements of pressure taps on the shell roof

3. HIGH-ORDER STATISTICS OF WIND PRESSURE

Skewness and kurtosis are the two main parameters used to measure non-Gaussian characteristics for a given process. For the data sample of pressure

coefficients with N data points sampled at discretized time instants $t_j, j=1, \dots, N$, the skewness and kurtosis can be estimated statistically as follows:

$$\gamma_3 = \frac{1}{N} \sum_{j=1}^N \left[\frac{C_{pi}(t_j) - C_{pi,mean}}{C_{pi,std}} \right]^3 \quad (3)$$

$$\gamma_4 = \frac{1}{N} \sum_{j=1}^N \left[\frac{C_{pi}(t_j) - C_{pi,mean}}{C_{pi,std}} \right]^4 \quad (4)$$

where $C_{pi,mean}$ and $C_{pi,std}$ are the mean and standard deviation, respectively, of the pressure coefficient.

As reported by Choi and Sweetman (2010), a skewness–kurtosis combination for a random process will satisfy the following practical limit:

$$\gamma_4 \geq \gamma_3^2 + 1 \quad (5)$$

The monotonic region, which defines the applicable range for the application of the Hermite polynomial model, could be expressed as (Winterstein and MacKenzie 2012)

$$\gamma_4 \geq (1.25\gamma_3)^2 + 3 \quad (6)$$

It is clear that γ_4 should be greater than 3. Therefore, the Hermite polynomial model (HPM) proposed in the work of Yang et al. (2013) and Peng et al. (2014) is only applicable for softening non-Gaussian processes. Fig. 2 presents a scatter plot of paired values of skewness and kurtosis in moment space for measured net pressure coefficients. While the parabolic dashed curve shown in Fig. 3 represents the practical limit given by Eq. (5), the parabolic solid curve indicates the monotonic region of Eq. (6). As shown in Fig. 2, the skewness–kurtosis combinations of all measured pressure coefficients on the roof are above this parabolic limit. As expected, a considerable number of points fall out of the monotonic region and below the line of $\gamma_4 = 3$, indicating the noticeable existence of hardening wind pressure processes.

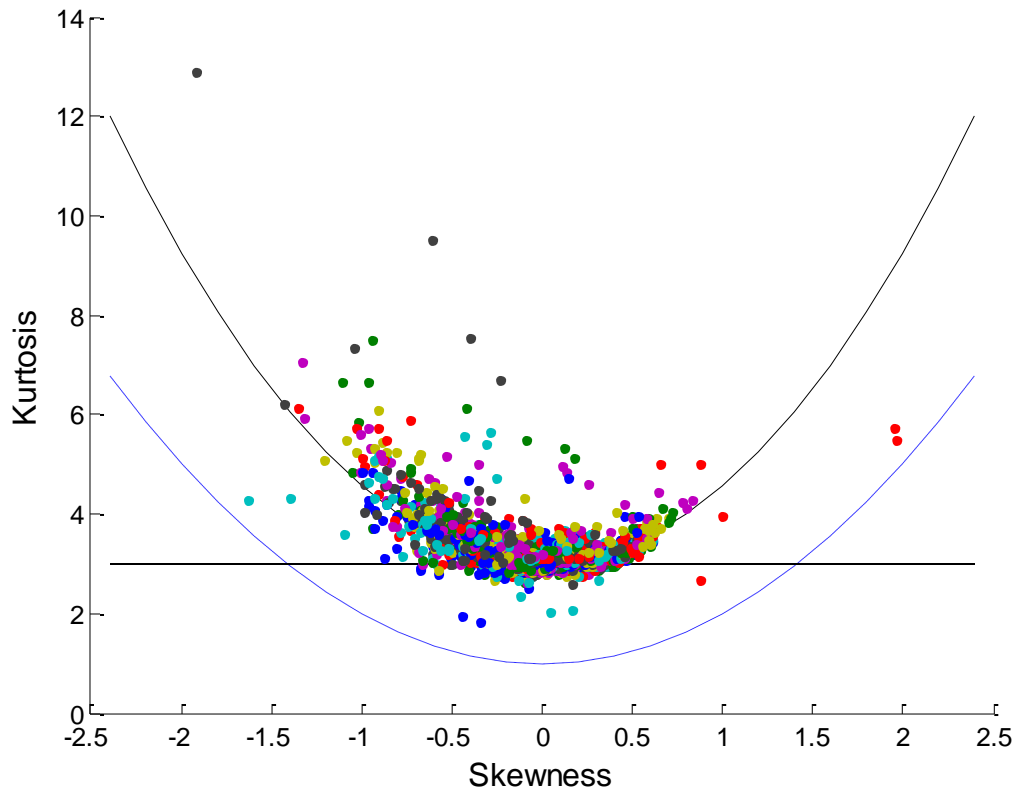
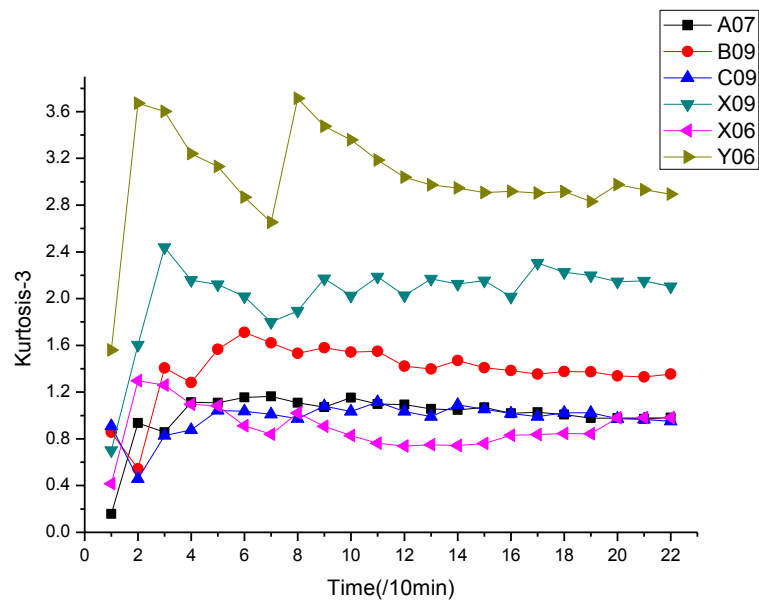
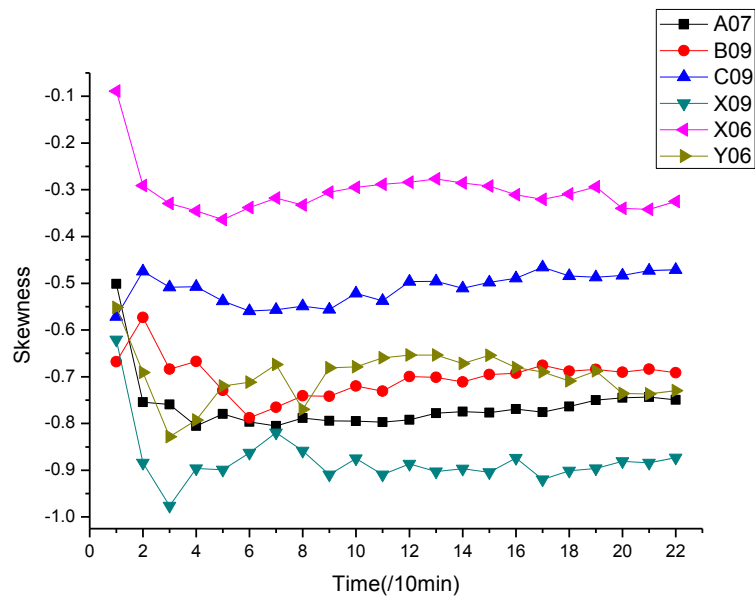


Fig. 3 Paired values of skewness and kurtosis from all taps

The sensitivities of skewness and kurtosis to the record duration were presented in Figs. 4 and 5. Each data point in Figs. 4 and 5 is an estimation based on increasing data record with a 10-minute step. Fig. 4 presents high-order moments for six typical softening net pressure processes, identified at the pressure tap locations, i.e., A07, B09, C09, X09, X06 and Y06 (denoted as circle in Fig. 2) under 0-degree wind without coal. The estimated values of skewness and kurtosis are obviously fluctuated with the varying record duration. With the increasing of record duration, the estimations of high-order moments become stable and converge to particular values. Fig. 5 presents skewness and kurtosis for six selected hardening pressure processes, identified at the pressure tap locations, i.e., H08, I08, J08, K07, L06 and M08 (denoted as square in Fig. 2) under 0-degree wind without coal. Similar to softening processes, the estimated values of skewness and kurtosis vary significantly with the increasing of record duration. It was found that the high-order moments, i.e., skewness and kurtosis, are sensitive to the time duration of data samples. That is to say, it may be difficult to obtain reliable estimations of high-order moments only with short-term time history samples. This observation indicates that the moment-based translation method may not appropriate for extreme value analysis of non-Gaussian wind effects with short-term time history samples.

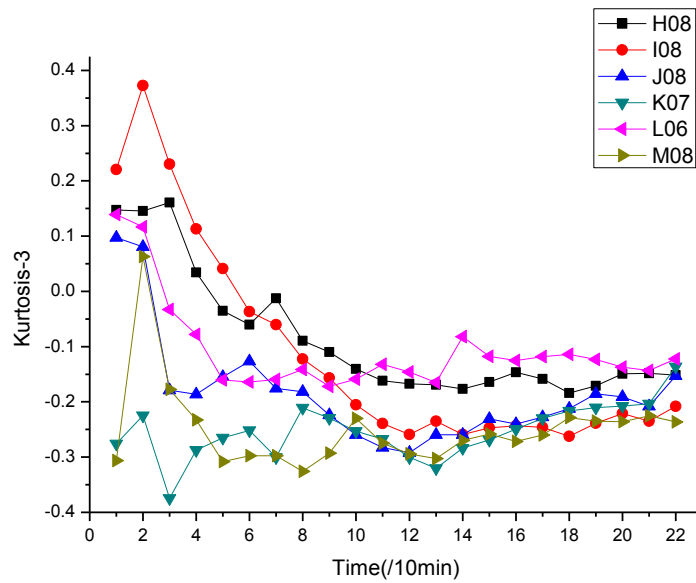


(a)

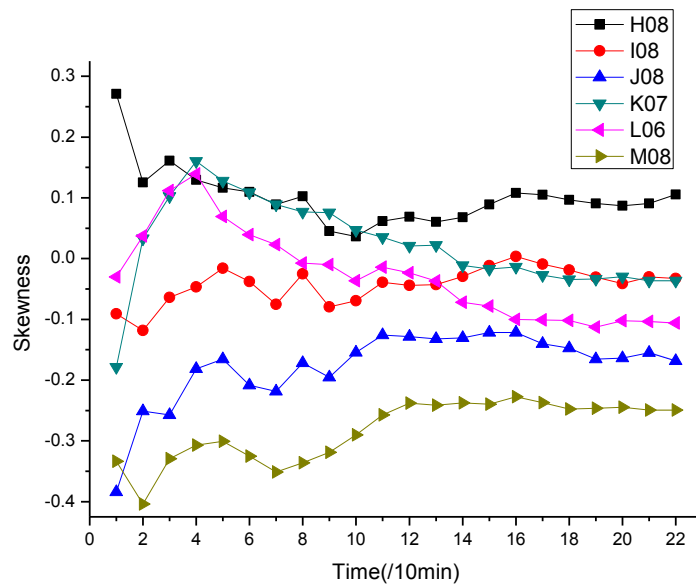


(b)

Fig. 4 Estimated skewness and kurtosis for six softening processes



(a)



(b)

Fig. 5 Estimated skewness and kurtosis for six hardening processes

4. A MIXTURE MODEL FOR PARENT PRESSURE DISTRIBUTION

The point-to-point CDF mapping approaches, i.e., the SS and TPP methods, require the parent distribution models. In this paper, a flexible mixture model for analyzing extreme pressure coefficients has been adopted. The flexible mixture model includes a non-parametric smooth kernel density estimator below some threshold accompanied with the generalized Pareto distribution (GPD) model for the upper tail above the threshold. This mixture model avoids the need to assume a parametric form for the bulk distribution, and captures the entire distribution function below the threshold

using a smooth flexible non-parametric form. The expression for GPD is

$$F_{GPD}(x) = \Pr(X \leq x | X > u) = \frac{F_X(x) - F_X(u)}{1 - F_X(u)} = 1 - \left[1 + \frac{\xi(x-u)}{\sigma} \right]^{-1/\xi} \quad (7)$$

where u denotes the chosen threshold; σ and ξ are scale and shape parameters, respectively. The inference of GPD parameters can be performed using either maximum likelihood or method of moments applied to the data beyond the selected tail-index u (Harris 2005). The GPD model provides an approximation to parent CDF above a selected high threshold u as

$$F_X(x) = F_X(u) + F_{GPD}(x)[1 - F_X(u)], \quad x \geq u \quad (8)$$

The original version of the TPP method can be modified by adopting the proposed mixture model for parent pressure distribution. The modified version was denoted as ParTPP for comparative purposes.

5. COMPARATIVE PERFORMANCE STUDY FOR NON-GAUSSIAN PEAK FACTORS

For a zero-mean process, the so-called peak factor can be defined as the ratio of the mean extreme value to the standard deviation value of the process. Four different methods/schemes were employed in this paper to calculate peak factors of wind pressure processes. The SS procedure, the TPP method and its new version of ParTPP represent the common CDF mapping approach. The Hermite model approach was implemented by employing two non-Gaussian peak factors for softening processes and hardening processes, respectively. For a softening process, Kwon and Kareem (2011) revisited the non-Gaussian peak factor and developed the following expression of the Hermite moment-based non-Gaussian peak factor (Kareem and Zhao 1994; Kwon and Kareem 2011):

$$\begin{aligned} \bar{x}_{ng} = \alpha \left\{ \left(\beta + \frac{\gamma}{\beta} \right) + h_3 \left(\beta^2 + 2\gamma - 1 + \frac{1.98}{\beta^2} \right) \right. \\ \left. + h_4 \left[\beta^3 + 3\beta(\gamma - 1) + \frac{3}{\beta} \left(\frac{\pi^2}{6} - \gamma + \gamma^2 \right) + \frac{5.44}{\beta^3} \right] \right\} \end{aligned} \quad (9)$$

where $\gamma = \text{Euler's constant} (\approx 0.5772)$; $\beta = \sqrt{2 \ln(\nu_0 T)}$; $\nu_0 = \text{mean zero upcrossing rate of a standardized non-Gaussian process } x(t)$ (obtained from a general non-Gaussian process $X(t)$ as $x(t) = [X(t) - \mu_X] / \sigma_X$, where $\mu_X = \text{mean value of } X(t)$, $\sigma_X = \text{the standard deviation of } X(t)$); $T = \text{time duration}$; α, h_3, h_4 are parameters of the moment-based Hermite model (Winterstein 1988), which gives a transformation from a standard Gaussian process $y(t)$ to the standardized non-Gaussian process $x(t)$,

$$x = \alpha \left[y + h_3(y^2 - 1) + h_4(y^3 - 3y) \right] \quad (10)$$

where the parameters h_3 and h_4 control the shape of the distribution, while the parameter $\alpha = (1 + 2h_3^2 + 6h_4^2)^{-1/2}$ is the scaling factor. In the "softening" case, that is, $\gamma_4 > 3$, the second-order and third-order approximate analytical solutions are available

(Winterstein 1988; Winterstein and Kashef 2000). New expressions for h_3 and h_4 were recently suggested by Yang et al. (2013)

$$h_3 \approx 0.1967\gamma_3 - 0.01646\gamma_3\gamma_4 + 0.01809\gamma_3^3 \quad (11)$$

$$h_4 \approx -0.0721 + 0.03176\gamma_4 - 0.02942\gamma_3^2 - 0.00179\gamma_4^2 + 0.002348\gamma_3^2\gamma_4 \quad (12)$$

Eqs. (9), (11) and (12) establish a way to evaluate non-Gaussian peak factors of softening processes, denoted as NGS.

Based on the work of Choi and Sweetman 2010, an analytical solution for the non-Gaussian peak factor of a hardening process can be obtained as (Huang et al. 2014)

$$g_{NGH} = \frac{-h_3}{3h_4} + \frac{1}{3}\sqrt{3a_1 - a_2^2} \times \left[\left(C_0 + \sqrt{C_0^2 + 1} \right)^{1/3} - \left(C_0 + \sqrt{C_0^2 + 1} \right)^{-1/3} \right] \quad (13)$$

where $a_1 = (1 - 3h_4)/h_4$, $a_2 = h_3/h_4$ and C_0 are three parameters depending only on the Hermite coefficients h_3 and h_4 ; C_0 is given as follows:

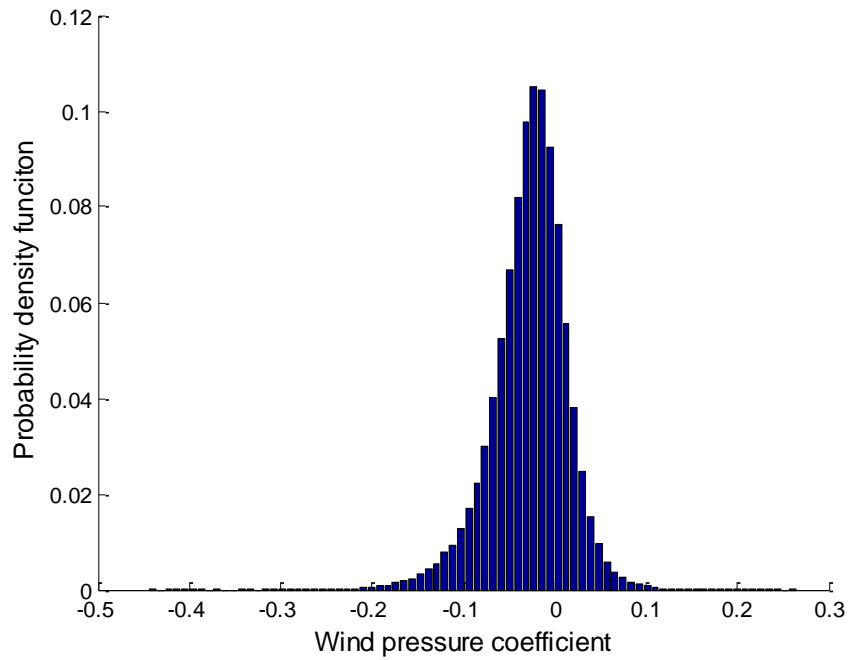
$$C_0 = \frac{-27(-\beta - \gamma / \beta - h_3)/h_4 + 9a_1a_2 - 2a_2^3}{54} \times \left(\frac{9}{3a_1 - a_2^2} \right)^{1.5} \quad (14)$$

The use of Eq. (13) to calculate the non-Gaussian peak factor of a hardening process is denoted as NGH.

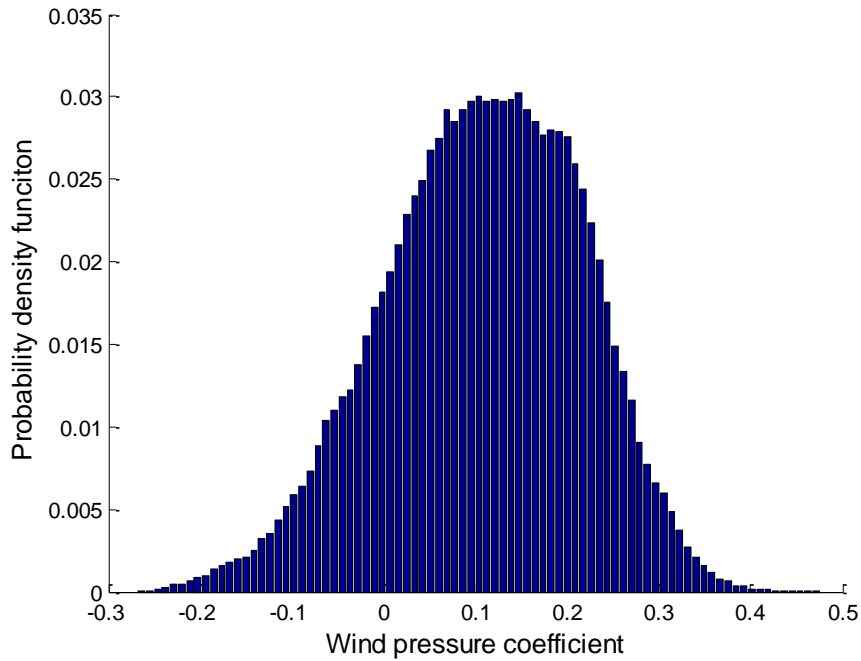
The time series obtained at two pressure tap locations (Y06 and M08, as shown in Fig.2) are analyzed in this section. Fig. 6 shows the data histogram (HIST) from Taps Y06 and M07. While the pressure time series measured at Tap Y06 represents a typical softening load process with a skewness of -0.73 and a kurtosis of 5.89, the time series at Tap m08 is a hardening process with a skewness of -0.25 and a kurtosis of 2.73. The histogram reveals that the distribution of M08 has bimodal property and the kurtosis estimated is less than 3. In fact, all the processes with bimodal property have a kurtosis less than 3 (DeCarlo 1997). The non-Gaussian peak factor results were respectively calculated by four methods, i.e., SS, TPP, ParTPP and NGS(or NGH), and were presented in Figs. 7 and 8. The total duration of pressure time history data for direct statistical analysis was 220-minute in full-scale, including 22 samples of 10-minute pressure coefficient data. The expected maximum (peak factor) of pressure coefficients for 10-minute duration were then computed by averaging the 22 observed maximum pressure coefficients over the 22 samples of 10-minute records. The direct statistical analysis (DSA) could provide benchmark results for weighting up other methods.

Fig. 7 presents non-Gaussian peak factors of a softening process from Tap Y06 under 0-degree wind for the case of without coal. The 22 peak factor results were obtained with varying record duration corresponding to each method. That is to say, the data used for calculating peak factors is starting from the first 10-minute duration to two 10-minute durations, up to 220-minute duration. The moment-based translation method, i.e., NGS, shows obvious sensitivity to data duration in the estimation of peak factors. The fluctuating pattern of NGS in Fig. 7 seems quite similar to the variation pattern of estimated kurtosis of Y06 in Fig. 4(b). For a softening process, NGS also overestimates the non-Gaussian peak factors compared to the DSA result. On the other hand, the peak factor results from the CDF mapping approach (i.e., TPP, ParTPP and SS) exhibit

less variation along the time axis. The TPP and ParTPP methods are capable of giving the best estimation of non-Gaussian peak factors compared to other two methods.



(a) Tap Y06



(b) Tap M08

Fig. 6 The data histograms for pressure coefficient of Tap Y06 and M08

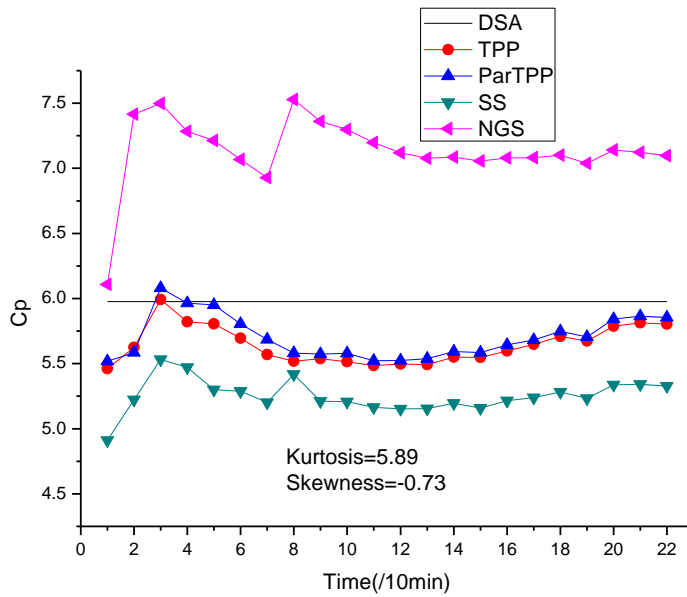


Fig. 7 Comparison of estimated non-Gaussian peak factors for Tap Y06

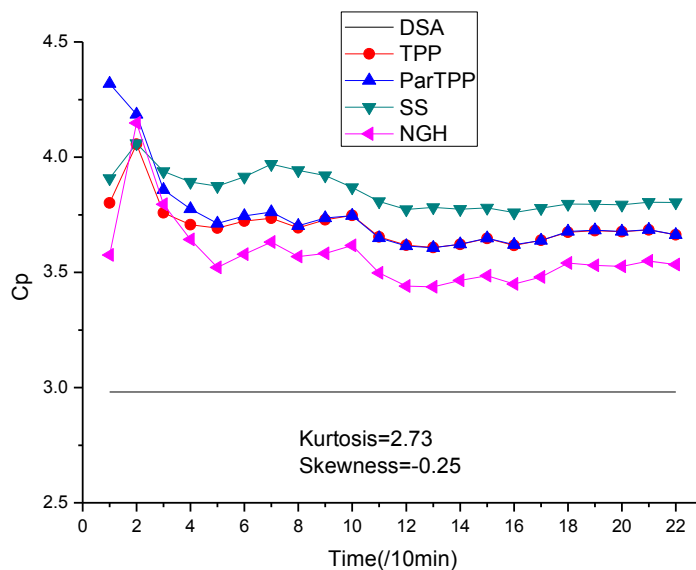


Fig. 8 Comparison of estimated non-Gaussian peak factors for Tap M08

Fig. 8 presents non-Gaussian peak factors of a hardening process from Tap M08 under 0-degree wind for the case of without coal. The moment-based translation method, i.e., NGH, also shows strong sensitivity to data duration in the estimation of peak factors. For a hardening process, all four methods overestimate the non-Gaussian peak factors compared to the DSA benchmark result. In terms of accuracy, NGH with

Eq. (13) is able to offer the best result of non-Gaussian peak factor of the hardening process. The ParTPP does not appear to achieve an improvement over the original TPP method.

6. CONCLUSIONS

In this paper, high-order moments and peak factors of non-Gaussian pressure process are investigated based on the wind tunnel experiments of a cylindrical reticulated roof structure. The focus is put on the sensitivity of non-Gaussian statistical estimation to the time duration of data record. It was found that high-order moments of pressure coefficient data show strong sensitivity to the record duration. Such observation renders the moment-base translation method much more uncertainty in the estimation of peak wind loads with short-term time history samples. For softening pressure processes, the CDF mapping approaches, including the SS procedure and the TPP method, demonstrate their advantages of stability and accuracy over the moment-based translation method in calculating non-Gaussian peak factors. However, for hardening pressure processes, although the TPP method is also capable of giving the good estimation of non-Gaussian peak factors, the moment-based method using recently proposed Eq. (13) is able to achieve the best estimation of peak factors among four methods compared to the DSA benchmark result. The ParTPP considering the mixture distribution model does not seem helpful in further improving the accuracy of the current TPP method.

ACKNOWLEDGEMENTS

The work described in this paper was partially supported by the Ministry of Transport of PR China (Project No. 2011318223170) and the Scientific Plan Project of Zhejiang Province of China (Project No. 2012C21059).

REFERENCES

- Chen, X. (2014). "Extreme value distribution and peak factor of crosswind response of flexible structures with nonlinear aeroelastic effect." *Journal of Structural Engineering*(in press).
- Choi, M., and Sweetman, B. (2010). "The Hermite moment model for highly skewed response with application to tension leg platforms." *Journal of Offshore Mechanics and Arctic Engineering*, **132**, 021602.
- DeCarlo L.T. (1997). "On the meaning and use of kurtosis." *Psychological Methods*, **2**(3), 292-307.
- Ding, J., and Chen, X. (2014). "Assessment of Methods for Extreme Value Analysis of Non-Gaussian Wind Effects with Short-Term Time History Samples." Submitted to *Engineering Structures*.
- Harris, I. (2005). "Generalised Pareto methods for wind extremes: usefull tool or mathematical mirage?" *Journal of Wind Engineering and Industrial Aerodynamics*, **93**, 341-360.

- Huang, M.F., Lou, W.J., Chan, C.M., et al. (2013), "Peak Distributions and Peak Factors of Wind-Induced Pressure Processes on Tall Buildings.", *J. Eng. Mech.*, **139**(12), 1744-1756.
- Huang, M.F., Lou, W.J., Pan, X.T., et al. (2014), "Hermite extreme value estimation of non-Gaussian wind load process on a long-span roof structure.", *J. Struct. Eng.* DOI: **10.1061/(ASCE)ST.1943-541X.0000962**.
- Kwon, D., Kareem, A. (2011), "Peak factors for non-Gaussian load effects revisited", *J. Struct. Eng.*, ASCE, **137**(12), 1611-1619.
- Kareem, A., Zhao, J., 1994. Analysis of non-gaussian surge response of tension leg platforms under wind loads. *J. Offshore Mech. Arct. Eng.* **116**, 137–144.
- MacDonald, A.; Scarrott, C.J.; Lee, D.; Darlow, B.; Reale, M. & Russell, G. (2011a). A flexible extreme value mixture model, *Comp. Statist. Data Anal.*, **55**, 2137–2157.
- MacDonald, A.; Scarrott, C.J. & Lee, D.S. (2011b). Boundary correction, consistency and robustness of kernel densities using extreme value theory. Available from: <http://www.math.canterbury.ac.nz/c.scarrott>.
- Peng, X., Yang, L., Gavanski, E., et al. (2014), "A comparison of methods to estimate peak wind loads on buildings", *J. Wind Eng. Ind. Aerodyn.*, **126**, 11-23.
- Sadek, F., Simiu, E., 2002. Peak non-Gaussian wind effects for database-assisted low-rise building design. *J. Eng. Mech.* **128**, 530–539 (Compendex).
- Tieleman, H.W., Elsayed, M.A.K., Hajj, M.R., 2006. Peak wind load comparison: theoretical estimates and ASCE 7. *J. Struct. Eng.* **132** (7), 1150–1157.
- Winterstein, S.R. (1988). "Nonlinear vibration models for extremes and fatigue." *Journal of Engineering Mechanics*, ASCE **114**, 1772–1790.
- Winterstein, S.R., Kashef, T., 2000. Moment-based load and response models with wind engineering applications. *J. Sol. Energy Eng., Trans. ASME* **122** (3), 122–128.
- Yang, L., Gurley, K.R., Prevatt, D.O., 2013. Probabilistic modeling of wind pressure on low-rise buildings. *J. Wind Eng. Ind. Aerodyn.* **114** (0), 18–26.